Regional-scale tuned model to estimate the dissolved organic carbon in Barra Bonita reservoir from OLI/Landsat-8 images

Enner Alcântara[1]
Nariane Bernardo[2]
Thanan Rodrigues[2]
Fernanda Watanabe[2]

[1]Universidade Estadual Paulista – Unesp, Departamento de Engenharia Ambiental
12247-004 - São José dos Campos – SP, Brasil.
enner.alcantara@ict.unesp.br

[2] Universidade Estadual Paulista – Unesp - Departamento de Cartografia
19060-900 - Presidente Prudente – SP, Brasil.
{narianebernardo, twalesza, fernandasyw}@gmail.com

Abstract. Through exchange of heat and water with the atmosphere inland waters affect climate at the regional scale and play an important role in the global carbon cycle. Therefore there is a need to develop methods and models for mapping inland water carbon content to understand the role of lakes in the global carbon cycle. The colored dissolved organic matter (CDOM) has a strong correlation with dissolved organic carbon (DOC) and can be studied using remote sensed images. In this work, we developed an empirical model to estimate the DOC concentration by using the absorption coefficient of CDOM (a_{CDOM}). The a_{CDOM} was estimated through band ratio index and validated with in situ data. The empirical adjusted model to estimate the DOC was applied to a series of OLI/Landsat-8 images. The results showed a good relationship between the a_{CDOM} at 412 nm ($a_{CDOM412}$) and the ratio between OLI band 1 and OLI band 3, but the validation results showed a normalized root mean square error (NRMSE) of about 37.89%. The $a_{CDOM412}$ obtained in laboratory was used to establish a relationship between $a_{CDOM412}$ and DOC. The DOC spatial distribution was then obtained and the concentration varied from 22 to 52 mg.l^{-1} during the year of 2014.

Keywords: carbon content, inland water, bio-optical model, and cascading reservoirs, conteúdo de carbono, águas interiores, modelo bio-óptico, reservatórios em cascata.

1. Introduction

Colored dissolved organic matter (CDOM) is a photoactive component of dissolved organic carbon (DOC) and is often viewed as a reliable tracer of DOC (Zhu et al. 2014). According to Hoge and Lyon (2002) in freshwater environments the optical properties of CDOM-laden water are affected by microbiological assemblages and suspended substances. CDOM absorptivity in these aquatic systems can be quite high with absorption as high as 20 m^{-1} at 440 nm (Brezonik et al. 2005). There is a strong correlation between CDOM and DOC in humic water bodies where is expected that both are fluctuating synchronously (Tranvik et al. 2009); therefore CDOM is often used as a proxy to map DOC content in water (Kutser et al. 2009).

Inland waters affect the climate at regional scale and plays an important role in the global carbon cycle. Anthropogenic activities altering the aquatic landscape, mainly through the construction of large hydroelectric reservoirs will also contribute to modify the carbon balance. Inland waters are also considered sites of transport, transformation and storage of considerable amount of carbon from terrestrial environment (Tranvik et al. 2009). Therefore understanding the role of inland water in the global carbon cycle requires reliable estimates of DOC, which creates the need to develop remote sensing methods for mapping lake carbon content.

Remote sensing provides an effective approach to estimate the CDOM absorption coefficient (a_{CDOM}) in a large spatial scope. The estimation of a_{CDOM} via remote sensing could be a valuable tool to study ecological changes as well as carbon cycling at global scales (Slonecker et al. 2016). A summary of bio-optical models often used to estimate the a_{CDOM} can be accessed in Zhu et al. (2014) and the factors that affect the measurement of CDOM from remote sensing are in Brezonik et al. (2015).

According to Toming et al. (2013) there is a lack of data about the DOC-CDOM relationship in eutrophic inland waters, where autochthonous DOC may form a considerable fraction of the total DOC pool when compared to allochthonous DOC. Autochthonous DOC is produced by phytoplankton and other photosynthetic organisms and the allochthonous from vascular plants and soil organic matter of the catchment area (Toming et al. 2016).

In this context, the aim of this work was to calibrate and validate a regional model for estimating the DOC concentration from OLI/Landsat-8 images in a meso-to-hypertrophic reservoir.

2. Materials and Methods
2.1 Study Area

Barra Bonita hydroelectric reservoir (BB reservoir) (22° 31' 10" S and 48° 32' 3" W) lies in the middle course of the Tietê River, São Paulo State, Brazil (Figure 1). The BBHR is situated in a transitional region between tropical and subtropical climate, characterized by a dry (May – October) and a wet (November – April) periods.
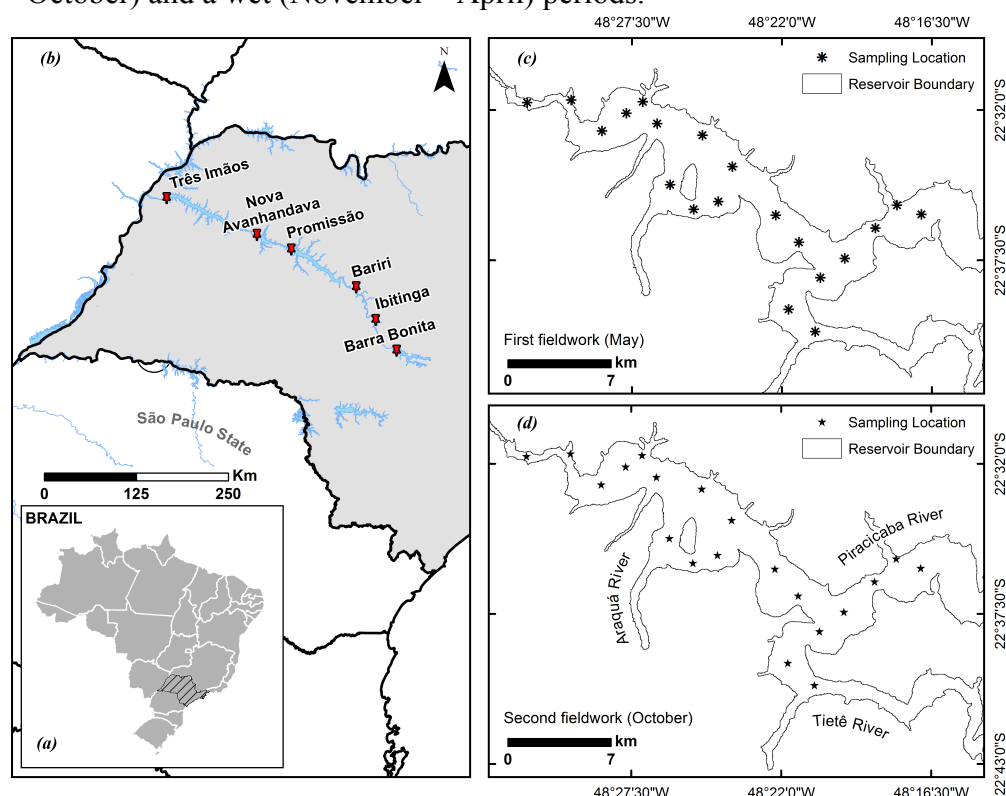

Figure 1: Location of study area (*a*) Brazil, with São Paulo State highlighted; (*b*) Tietê River and the cascade of reservoirs (from upstream to downstream: Barra Bonita (study area), Ibitinga, Bariri, Promissão, Nova Avanhandava, and Três Irmãos). The sampling locations for the first fieldwork (May) and second fieldwork (October) can be seen in (*c*) and (*d*), respectively. Source: Alcântara et al. (2016).

The maximum depth is 25 m, with an average of 10.2 m. The water retention time varies from 30 days (austral summer) to 180 days (austral winter), while the flow range is of 1,500

m^3 s^{-1} in the austral summer (wet season) to 200 m^3 s^{-1} in the austral winter. BB reservoir is characterized as highly productive waters and presents a species richness and high concentration of phytoplankton. The BB reservoir is eutrophic due to a high load of wastewater and fertilizers coming from the lower Tietê River (Watanabe et al. 2016).

2.2 Fieldwork

Two campaigns were carried out from 5 to 8 May 2014 and from 13 to 17 October 2014. The sampling stations from both fieldworks (n=25) were defined as methodology proposed by Rodrigues et al. (2016).

2.3 Radiometric data

In situ radiometric measurements were made using three TriOS hyperspectral radiometers: two ARC-VIS sensors with a 7° field-of-view in order to measure radiance and one ACC-VIS sensor with a cosine collector to measure irradiance. Both ARC and ACC sensors have 3.3 nm of spectral sampling, work in a wavelength ranging from 320 nm to 950 nm, use an integration time of 4 ms to 8 s, and an operation temperature ranging from -10°C to +50°C (TriOS, Oldenburg, Germany). Radiances (total radiance – L_t; and diffuse radiance – $L_{sky,}$ both in W m^{-2} sr^{-1}) and downwelling irradiance data (E_d (0$^+$), in W m^{-2}) were measured in an azimuth angle of 90° in relation to the Sun's direction in order to minimize the specular reflection and boat shadow (Mobley 1999). To avoid shadow from the instrument the fieldwork followed the geometry suggested by Mueller (2003). The hyperspectral measurements allowed computing the remote sensing reflectance (R_{rs}, units in sr^{-1}) above water, by using Equation 1.

$$R_{rs}\left(\theta,\phi,\lambda,0^+\right) = \frac{L_t\left(\theta,\phi,\lambda,0^+\right) - 0.028 \times L_{sky}\left(\theta,\phi,\lambda,0^+\right)}{E_d\left(\theta,\phi,\lambda,0^+\right)} \tag{1}$$

where θ is the azimuthal angle (in degrees), ϕ is the zenithal angle (in degrees), λ is the wavelength (in nm), and 0$^+$ indicates that measurements were made just above the water surface.

To simulate the $R_{rs}(\lambda)$ signals that would be recorded by the satellite sensor at each channel centered at wavelength λ, weighted averages of each R_{rs} spectrum were calculated by using as weights the spectral band responses of OLI (Barsi et al. 2014), as given below (Equation 2).

$$R_{rs\_s}(\lambda) = \frac{\sum_{\lambda} R_{rs}(\lambda) \times S(\lambda)}{\sum_{\lambda} S(\lambda)} \tag{2}$$

where $S(\lambda)$ is the OLI spectral response function, and $R_{rs\_s}(\lambda)$ is the simulated R_{rs}.

2.4 Colored dissolved organic matter absorption coefficient (a_{CDOM})

Water samples were filtered through a nylon membrane Whatman with 0.22 μm pore size and 47 mm diameter to measure the CDOM absorbance (A_{CDOM}). The filtrates were stored and kept cool in the dark until the analysis. The samples were measured at room temperature using a quartz cuvette with 10 cm optical path. The measurements were conducted in a spectral range of 280-800 nm using a 2600 UV-Vis spectrophotometer (Shimadzu, Kyoto, Japan) with a single beam and Milli-Q water was used as blank reference. From the A_{CDOM}, a_{CDOM} was calculated by using Equation 3 (Bricaud *et al.*, 1981).

$$a_{CDOM} = 2.3 \frac{A_{CDOM}(\lambda)}{l} \tag{3}$$

where $A_{CDOM}(\lambda)$ is the absorbance at wavelength (λ) and l is the cuvette path length in meters (Bricaud et al., 1981).

2.5 a_{CDOM} and DOC algorithm development

Three empirical models were tested in order to estimate the a_{CDOM} in BB reservoir, the D'Sa and Miller (2003), Maninno et al. (2008) and Ficek et al. (2011) models. These models were recalibrated using the R_{rs} *in situ* data and the a_{CDOM} obtained in laboratory. The algorithm validation was performed using comparisons with *in situ* measurements obtained in the fieldworks. Root Mean Squared Error (RMSE; Equation 4), Normalized Root Mean Squared Error (NRMSE; Equation 5), bias (Equation 6) and the coefficient of determination (R^2) were used to evaluate the performance of the algorithms.

$$RMSE = \sqrt{\frac{1}{n}\sum_{i=1}^{n}(x_i^{estimated} - x_i^{measured})^2} \tag{4}$$

$$NRMSE = \frac{RMSE}{x_{max}^{measured} - x_{min}^{measured}} \times 100 \, (\%) \tag{5}$$

$$bias = \frac{1}{n}\sum_{i=1}^{n}(x_i^{estimated} - x_i^{measured}) \tag{6}$$

Once we have identified the more suitable a_{CDOM} model the next step was to establish an empirical relationship between the a_{CDOM} and DOC. The empirical model to estimate DOC based on a_{CDOM} was then applied to OLI/Landsat-8 images.

2.6 OLI/ Landsat-8 images processing

The developed algorithm to predict the DOC was applied in five OLI/Landsat-8 images (path/row 220/76) from 2014 (level 1 product). The images were acquired on 31 January, 11 September, 13 October, 29 October, and 16 December and available on United States Geological Survey (USGS) site (www.earthexplorer.com). The signal registered by a remote sensor is influenced by the atmospheric attenuation (scattering and absorption of gases and molecules), and it is affected by the differences in geometry and illumination conditions.

Then, it is essential to differentiate these interferences from the real radiometric signal from the targets. Based on this, the radiometric normalization process was conducted using the Iteratively Reweighted Multivariate Alteration Detection - IR-MAD (Canty et al., 2004). To conduct the IR-MAD processing, the reference image was atmospherically corrected by using FLAASH (Fast Line-of-sight Atmospheric Analysis of Hypercubes, Adler-Golden et al., 1999) method. To apply the DOC algorithm, the surface reflectance (R_{SURF}) of each image were divided by π to convert them into R_{rs} (Moses et al. 2012).

3. Results and Discussion
3.1 a_{CDOM} and DOC algorithms

The most suitable model to estimate the a_{CDOM} was from D'sa and Miller model using 412 nm as reference ($a_{CDOM412}$). The $a_{CDOM412}$ model calibration was achieved using 14 samples and resulted in a $R^2 = 0.74$ with a linear adjustment (Figure 2a). The tuned model from D'sa and Miller uses OLI band 1 over OLI band 3 (OLI1/OLI3) as index and after the recalibration (Figure 2) using BB *in situ* data, the following equation was derived:

$$a_{CDOM\,412} = 0.9479 \times \frac{OLI1}{OLI3} + 1.563 \tag{7}$$

The $a_{CDOM412}$ model showed a linear pattern that is, when the index is higher, the $a_{CDOM412}$ is lower. Since the model is linear the values of $a_{CDOM412}$ higher than 1.5 m^{-1} can be estimated without losing the meaning, however the error can be increased. The tuned model to estimate $a_{CDOM412}$ was validated using 11 samples different from those used for calibration. The validation showed a NRMSE of 37.89% as we can see in Figure 2b. The model can be considered accurate in the range of 1.00-1.40 m^{-1} and above this value the model underestimate.
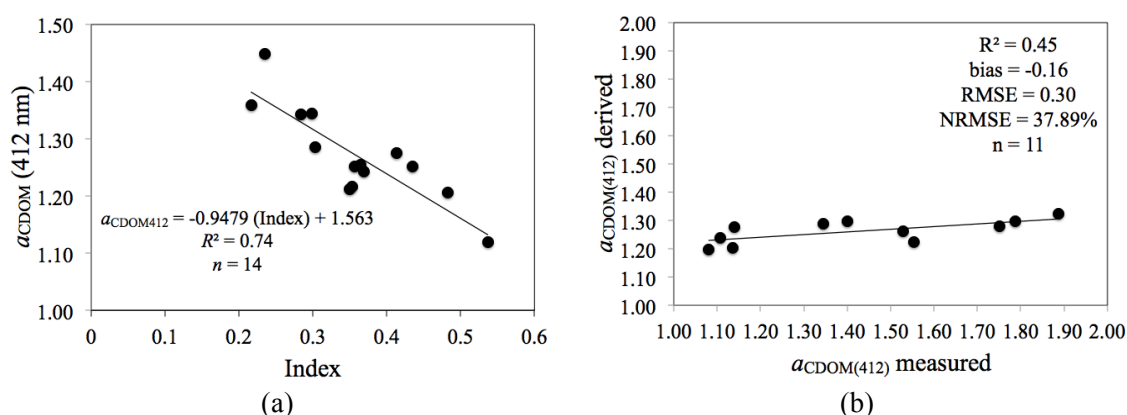

Figure 2: $a_{CDOM412}$ model calibration (a) and validation (b). Where index = OLI1/OLI3.

The 25 samples from May and October fieldworks were used to adjust an empirical model for estimating the DOC concentration from $a_{CDOM412}$. This model is displayed in the Figure 3 and the following equation was derived:

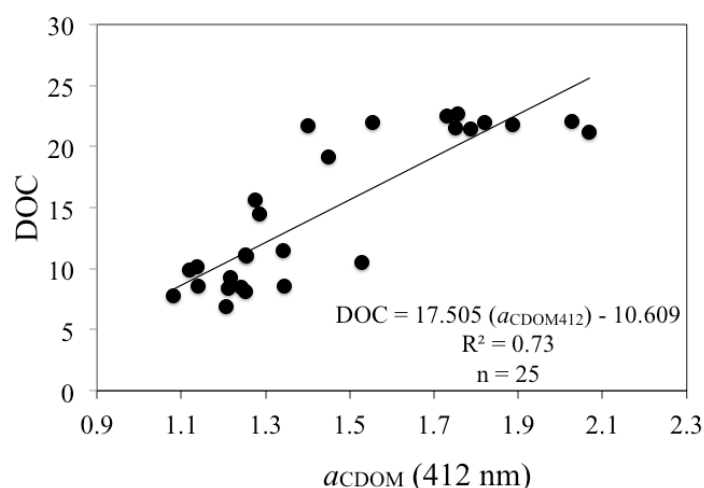$$DOC = 17.505 \times (a_{CDOM\,412}) - 10.609 \tag{8}$$

Figure 3: Relationship between DOC (mg.l^{-1}) and $a_{CDOM412}$ (m^{-1}).

The Figure 3 revealed that when the $a_{CDOM412}$ increases the DOC also increases. Furthermore, the errors in estimate DOC are higher when $a_{CDOM412}$ varies between 1.3 and 1.7 m^{-1} and lower with $a_{CDOM412}$ of 1.1 to 1.3 m^{-1}. Due to the DOC model simplicity the application to OLI/Landsat-8 images will be straightforward.

3.2 DOC algorithm application

The adjusted model to estimate DOC from $a_{CDOM412}$ was then applied to a series of images from 2014 (Figure 4). Since the terrestrial contribution of DOC is very important for inland water is expected that during the wet season the concentration of DOC is higher than during the dry season, which was showed in Figure 4. The higher values were found in the image from 16 December 2014 and the lower observed in the 30 January 2014 image. The main contribution of DOC to BB reservoir was the Tietê River. The spatial distribution of DOC on 11 September 2014 was more homogenous than in other months.
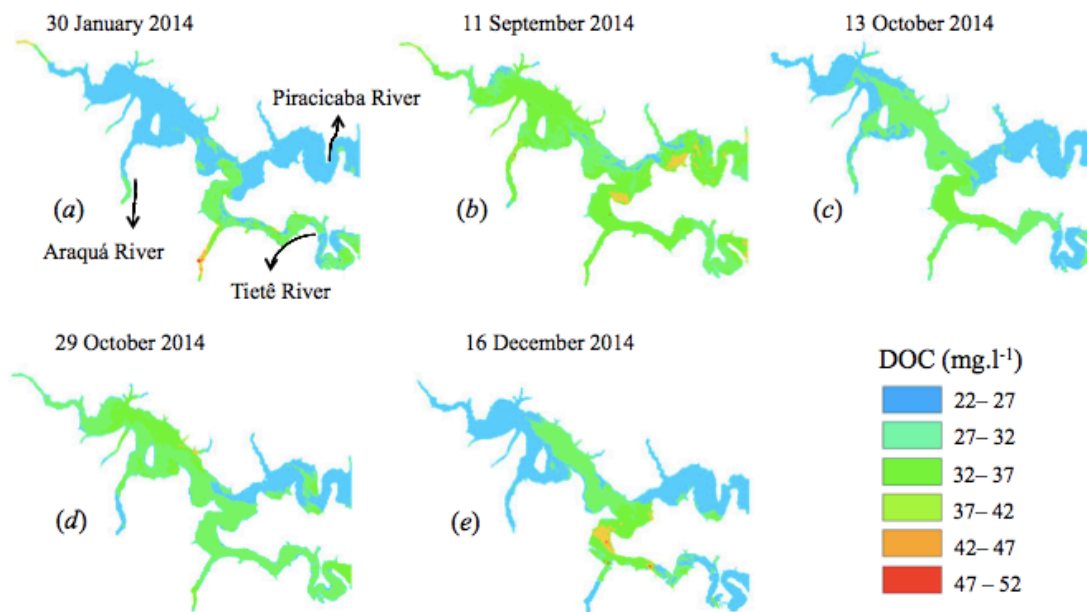

Figure 4: Spatial distribution of DOC in BB reservoir: (a) 30 January 2014, (b) 11 September 2014, (c) 13 October 2014, (d) 29 October 2014, and (e) 16 December 2014.

Watanabe et al (2015) using OLI/Landsat-8 images to predict the chlorophyll-*a* (Chl-*a*) concentration in BB reservoir found that the Piracicaba and Tietê Rivers were classified as hypertrophic both in May and in October. The Chl-*a* concentration in these months reached up to 500 mg m^{-3}. These authors also reported that in January the Chl-*a* concentration was higher in Tietê River than in Piracicaba River and the opposite occurred in October 2014. Since the phytoplankton degradation is one source of CDOM and DOC the knowledge about the Chl-*a* concentration distribution is essential.

Another source of CDOM and DOC is the surrounding terrestrial ecosystem. Prado and Novo (2015) used TM/Landsat-5 images to classify the land use and land cover in the BB reservoir watershed in the year of 2002. The results of this classification showed that the watershed was mainly occupied by pasture (29.35%), sugar cane (28.06%), natural vegetation (15.21%), bare soil (10.30%) and urban area (7.34%). There is a tendency in increasing the agriculture area in the watershed and therefore the CDOM and DOC will also increase. Since DOC has significant implications on our environment and climate change due to its important role in the carbon cycle, studying the CDOM distribution in aquatic systems will greatly improve our understanding about the dynamics of DOC and the impact on water quality (Tranvik et al. 2009).

4. Final considerations

Although there is a need to map the DOC concentration in inland waters, this task is still a challenge, mainly due to the need of having an accurate estimation of a_{CDOM} from R_{rs} data.

Until now the most accurate relationship obtained for inland waters were between a_{CDOM} and DOC; however, we might estimate a_{CDOM} firstly. Our results showed that a model to a_{CDOM} estimation for meso-to-hypertrophic waters is not easy to accomplish and therefore, the error of DOC estimation from satellite images may be reasonably high. The input of DOC from the catchment area needs to be quantified because as we saw in Figure 4, the DOC concentration tends to be higher during the wet season.

References
Adler-Golden, S.M.; Matthew, M.W.; Bernstein, L.S.; Levine, R.Y.; Berk, A.; Richtsmeier, S.C.; Acharya, P.K.; Anderson, G.P.; Felde, G.; Gardner, J.; Hoke, M.; Jeong, L.S.; Pukall, B.; Ratkowski, A.; Burke, H.H. Atmospheric correction for shortwave spectral imagery based on MODTRAN4. In: **SPIE Proceedings**, Imaging Spectrometry. 3753:61-69, 1999.

Alcântara, E.; Watanabe, F.; Rodrigues, T.; Bernardo, N. An investigation into the phytoplankton package effect on the chlorophyll-a specific absorption coefficient in Barra Bonita reservoir, Brazil. **Remote Sensing Letters**. 7:761-770, 2016.

Barsi, J.; Lee, K.; Kvaran, G.; Markham, B.; and J. Pedelty. The Spectral Response of the Landsat-8 Operational Land Imager. **Remote Sensing**. 6:10232–10251, 2014.

Brezonik, P.; Menken, K.D.; Bauer, M. Landsat-based remote sensing of lake water quality characteristics, including chlorophyll and colored dissolved organic matter (CDOM). **Lake and Reservoir Management**. 21:373-382, 2005.

Brezonik, P.; Olmanson, L.G.; Finlay, J.C.; Bauer, M.E. Factors affecting the measurement of CDOM by remote sensing of optically complex inland waters. **Remote Sensing of Environment**. 157:199-215, 2015.

Bricaud, A.; Morel, A.; Prieur, L. Absorption by dissolved organic matter of the sea (yellow substance) in the UV and visible domains. **Limnology and Oceanography**. 26:43-53, 1981.

Canty, M.J.; Nielsen, A.A.; Schmidt, M. Automatic radiometric normalization of multitemporal satellite imagery. **Remote Sensing of Environment**. 91:441-451, 2004.

D'Sa, E.J.; and Miller, R.L. Bio-optical properties in waters influenced by the Mississippi River during low flow conditions. **Remote Sensing of Environment**. 84:538-549, 2003.

Ficek, D.; Zapadka, T.; Dera, J. Remote sensing reflectance of Pomeranian lakes and the Baltic. **Oceanologia**. 53:959-970, 2011.

Hoge, F.E.; Lyon, P.E. Satellite observation of chromophoric dissolved organic matter (CDOM) variability in the wake of hurricanes and typhons. **Geophysical Research Letters**. 29. 2002.

Kutzer, T.; Tranvik, L.; Pierson, D. Variations in coloured dissolved organic matter between boreal lakes studied by satellite remote sensing. **Journal of Applied Remote Sensing**. 3:033538. 2009.

Mannino, A.; Russ, M.E.; Hooker, S.B. Algorithm development and validation for satellite-derived distribution of DOC and CDOM in the US Middle Atlantic Bight. **Journal of Geophysical Research – Oceans**. 113:19, 2008.

Mobley, C. D. Estimation of the remote-sensing reflectance from above-surface measurements. **Applied Optics.** 38:7442–7455, 1999.
Moses, W. J., Gitelson, A.A., Perk, R. L., Gurlin, D., Rundquist, D. C., Leavitt, B. C., Barrow, T. M., and P. Brakhage. Estimation of chlorophyll-a concentration in turbid productive waters using airborne hyperspectral data. **Water Research**. 46: 993–1004, 2012.

Mueller, J.L. In-water radiometric profile measurements and data analysis protocols. In: **Ocean Optics Protocols for Satellite Ocean Color Sensor Validation**, Revision 4, Volume III: Radiometric Measurements and Data Analysis Protocols; Mueller, J.L.; Fargion, G.S., & McClain, C.R. (Eds.). NASA Goddard Space Flight Space Center: Greenbelt, Maryland, USA, NASA/TM-2003-21621/Rev-Vol. III, pp.7-20. 2003.

Prado, R.B.; Novo, E.M.L.M. Modeling pollution potential input from the drainage basin into Barra Bonita reservoir, São Paulo – Brazil. **Brazilian Journal of Biology**. 75:314-323, 2015.

Rodrigues, T.; Guimarães, U.; Rotta, L.; Watanabe, F.; Alcântara, E.; Imai, N. Sampling design in reservoirs based on Landsat-8/OLI images: a case study in Nova Avanhandava reservoir (São Paulo State, Brazil). **Boletim de Ciências Geodésicas**. 22:303-323. 2016.

Slonecker, E.T.; Jones, D.K.; Pellerin, B.A. The new Landsat 8 potential for remote sensing of colored dissolved organic matter (CDOM). **Marine Pollution Bulletin**. 107:518-527. 2016.

Toming, K.; Tuvikene, L.; Vilbaste, S.; Agasild, H.; Kisand, A.; Viik, M.; Martma, T.; Jones, R.; Nõges, T. Contributions of autochthonous and allochthonous sources to dissolved organic matter in a large, shallow, eutrophic lake with a highly calcareous catchment. **Limnology and Oceanography**. 58:1259-1270. 2013.

Toming, K.; Kutser, T.; Tuvikene, L.; Viik, M.; Nõges, T. Dissolved organic carbon and its potential predictors in eutrophic lakes. **Water Research**. 102:32-40, 2016.

Tranvik, L.J.; et al. Lakes and reservoirs as regulators of carbon cycling and climate. **Limnology and Oceanography**. 54:2283–2297, 2009.

Watanabe, F.; Alcântara, E.; Rodrigues, T.; Imai, N.N.; Barbosa, C.; Rotta, L. Estimation of Chlorophyll-a Concentration and the Trophic State of the Barra Bonita Hydroelectric Reservoir Using OLI/Landsat-8 Images. **International Journal of Environmental Research and Public Health**. 12:10391-10417, 2015.

Watanabe, F.; Mishra, D.; Astuti, I.; Rodrigues, T.; Alcântara, E.; Imai, N.; Barbosa, C. Parametrization and calibration of a quasi-analytical algorithm for tropical eutrophic waters. **ISPRS Journal of Photogrammetry and Remote Sensing**. 121:28-47, 2016.

Zhu, W.; Yu, Q.; Tian, Y.Q.; Becker, B.L.; Zheng, T.; Carrick, H.J. An assessment of remote sensing algorithms for colored dissolved organic matter in complex freshwater environments. **Remote Sensing of Environment**. 140:766-778, 2014.